



Check for
updates



Research Article

Spatial Soil Salinity Assessment by Using Principle Component Analysis and Geospatial Techniques in Central Punjab, Pakistan

Sobia Khan¹, Aftab Ahmad Khan², Qudrat Ullah Khan³, Ali Raza Siddiqui^{4*}, Adeel Shahid⁴, Sumreen Anjum^{5*}, Shabana Nazeer⁶, Zain Mushtaq⁷, Syed Ayyaz Javed⁸, Muhammad Awais Piracha⁸, Farhat Bashir⁹, Munaza Batool¹⁰

¹ Water and Agriculture Division, National Engineering Services Pakistan (NESPAK), Lahore, 54000, Pakistan.

² Global Climate-Change Impact Studies centre (GCISC), Islamabad, Pakistan

³ Department of Soil Science, Gomal University Dera Ismail Khan, KPK, Pakistan

⁴ Department of Agriculture, Government College University Lahore, 54000, Pakistan

⁵ Institute of Botany, University of the Punjab, Lahore, Pakistan.

⁶ Soil and Water Testing Laboratory for Research, Lahore, 54000, Pakistan.

⁷ Department of Soil Science, University of the Punjab, Lahore, 54000, Pakistan.

⁸ Department of Soil and Environmental Sciences, College of Agriculture, University of Sargodha, 40100, Pakistan.

⁹ Soil and Water Testing Laboratory for Research, Dera Ghazi Khan, 03222, Pakistan.

¹⁰ Department of Soil and Environmental Sciences, Ghazi University, Dera Ghazi Khan, 32200, Pakistan.

ABSTRACT

Both natural and man-made soil salinity is a chief geological disaster in semi-arid and arid parts. In cultivated land, it has a negative impact on plant development and harvests, while in semi-arid and arid non-agricultural zones, due to subsidence, corrosion and groundwater quality, it affects urban structures, leading to additional soil erosion and land deprivation. The study was conducted at central Punjab, Pakistan with the aim to develop a baseline and to show the precision and accuracy of Geographic Information System (GIS) technology for delineating soil salinity in no data region. The samples of soil were gathered at deepness of 0-15 and 15-30 cm, and three factors (pH, Electrical Conductivity, and Sodium Adsorption Ratio) were analyzed in the laboratory. Landsat 8 OLI imagery were used for salinity indices development. A statistical index association was found between soil salinity noted in soil samples of field and 13 GIS-based salinity indices. The effect importance and model parameters for various soil salinity indices were assessed using regression model fitting. The data were divided into 3 categories: i) ground or field data, ii) brightness/intensity indicators, and iii) salinity indicators. Data were analyzed using principal component analysis (PCA). The results indicated that salinity indices were favorably related with ground data sets, but brightness/intensity indices had no significant relationship with ground or field data.

Keywords: Brightness indices, GIS, Landsat 8 OLI, PCA, Soil salinity.



Correspondence

Sumreen Anjum, Ali Raza Siddiqui,
sumreen38@gmail.com;
arsiddui@gcu.edu.pk

Article History

Received: October 22, 2024

Accepted: January 11, 2025

Published: January 27, 2025



Copyright: © 2024 by the authors.
Licensee: Roots Press,
Rawalpindi, Pakistan.

This article is an open access article distributed under the terms and conditions of the Creative Commons Attribution (CC BY) license:
<https://creativecommons.org/licenses/by/4.0>

INTRODUCTION

The content and soluble salts concentration in soil is known as soil salinity (Sarwar et al., 2017; 2018; 2022; De Boer and Radersma, 2011). Groundwater and soil salinization are serious risks to the agriculture in countries with low annual rainfall and high evaporation rates (Anjum et al., 2025a; Anjum et al., 2025; Song et al., 2017). Salinity related to soil is a worldwide concern, and rate at which the soil is becoming salty is worrying. According to Shahid et al., (2018), over 100 nations are dealing with soil salinity issues. Soil salinity is likely to worsen in the future,

owing mostly to climate change. Primary salinity was caused by normal geological processes including salt transport and redistribution. Salt deposition during weathering, as well as soil buildup by surface and groundwater, cause salinity. Secondary salinization is triggered by soil and water mishandling for a variety of causes (Anjum et al., 2025a; 2025b; Hussain et al., 2010). The estimated soil affected by salts differs. Commonly, it is estimated that 10% of world surface soils are covered with diverse types of salts, making it 1 billion hectares, around. It has also been assessed as a result of human intrusions that 77 million hectares has become saline, named as secondary salinization (Sarwar et al., 2019a; 2019b; 2021; Hillel, 2000). Irrigation through salinization and water logging into arid zones of several countries like Afghanistan, China and Pakistan, has affected huge regions of productive soils (Al-Khaier, 2003). There is 6.3 million hectares of brackish affected land in Pakistan. In terms of total extent of salt affected soils, Pakistan positions 8th in the biosphere (Martin et al., 2006).

Remote sensing (RS) is the source of footage evidence via electro-magnetic scale without any physical interaction. (Fussell et al., 1986). Lately the remote sensing applications are extensively used from plain soil or covered with plants in real time at various scales for salinity mapping and investigation. The outdated data gathering procedures including examination from laboratory and field studies for observing this main ecological issue are inadequate for preparation of further complete maps as mass of soil samples needed wide designs which make them costly and additional time consumption (Anjum et al., 2024; Allbed et al., 2014). Geographic information system (GIS) is the simple means for operating, storing and get into spatial data as an outcome of its capability to organize spatial and other data inside a private context (Rahman et al., 1997; Unwin, 1996; Estes et al., 1987). GIS and RS expertise have shown boundless potential for consistent observing and drawing of huge saline affected zones or ruined soils due to upgraded speed, accurateness and budget efficacy technologies. (Farifteh et al., 2006).

Tajgardan et al., (2010) observed salinity issue in Thailand and recognized several models of salinity including NDVI and different band ratios of Landsat for protruding and estimating the soil salinity. Their research displayed that Mid and Near Infrared has exposed worthy link with measured electrical conductivity (EC). Here are many statistical procedures used including spectral transformations e.g. PCA, Spectral vegetation indices using the NDVI/ Tassel-Cap transformation and further Landsat band percentages to classify and define soil salinity which are based on data attained from remote sensing (Eldeiry and García, 2004). Spectral Vegetation indices were mathematically merge from various spectral bands in visible and near infrared areas of electromagnetic spectrum. Soil spectral reflectance were affected by three major parameters which were color, roughness and amount of water (Bouman and Tuong, 2001). Elhag and Bahrawi (2017) evaluated that NDVI and its different derivatives were applied to detect crop water relationship by using Landsat 8 data along with that Principal Component Analysis.

Salinity related to soil is rapidly increasing, harming agricultural production in Punjab. Because of elevated sodicity and salinity in province Punjab, the ecological farming is under hazard. Salinity of soil is an imperative ecological issue in irrigated and/or canal parts that must be observed frequently to retain pathway of its infringement. Profitable growth of salt-prone soils requires inventive and feasible procedures, assessment tackles, and plan actions on a regular basis, such that new Geographic Information System and Remote Sensing methods can be effective methodologies.

The key objective of this investigate was to monitor spatiotemporal soil salinity change at the research sites by use of Landsat-8 satellite data. The detailed study objectives include; to know the level and concentration of salinity at research areas, to calculate the possible facts gained via GIS and RS for spatiotemporal soil salinity mapping, and to match the GIS-created map of soil salinity with Ground or field data for assessing the exactness and accurateness of GIS skill for describing diverse soil salinity classes.

MATERIALS AND METHODS

Study Area

This research study zone present at Rachna Doab bank and further stretched to the sites of Jarawala with geographic position 31°33'33" N 73°43'33" E, Chak Jhumra with geographic position 31°56' 78" N 73°18' 35" E, Chinot with geographic position 31°72' 00" N and 73°97' 89" E, and Pindi Bhattian with geographic position 31° 53' 45" N, 73°16'34" E located in Punjab province Punjab of Pakistan.

Research Area Climate

The study region has a semi-arid climate with subtropical continental influences. The region experiences two distinct seasons: a hot summer with a late monsoon and a mild winter. The hottest month is June, with temperatures reaching a maximum of 48°C and a minimum of 40°C. Conversely, January is the coldest month, with a maximum

temperature of 4.4°C and a minimum of -4.0°C. The normal yearly temperature ranges from 23.9°C to 32.3°C. The area receives an annual rainfall of approximately 380 to 400 mm, with the heaviest showers occurring in June and August (PMD, 2018).

Methodological Framework

The current work focuses on assessing the regression correlation and PCA among the ground truth data and the parallel salinity catalog value obtained from the satellite photos. Hence, accurate and reliable ground truth data was acquired and synced with satellite information.

Field Soil Sampling and Laboratory Analysis

Primary field study of suggested location was done and essential information was also gathered and examined for salinity attributes. A field experiment was carried out, during which a total of eighty soil samples were gathered in a random manner, with further consideration given to areas exhibiting visible signs of salinity. The GPS coordinates were also recorded as stated above. In three districts, the primary areas of the sample collecting were Tehsils of Jarawala, Chak Jhumra, Chinot, Pindi Bhattian, Gojra, Kamalia, and Toba Tek Singh. All collected soil samples were analyzed for pH, EC and SAR after passing from 2 mm sieve from Pindi Bhattian Soil Salinity Research Institute (SSRI) located in province Punjab of Pakistan.

Satellite Data Acquisition and Processing

Remote sensing data for December 2018 was obtained from the Landsat-8 OLI (Operational Land Imager) by downloading. The photos were georeferenced using WGS (World Geodetic System Application) 1984 standard data to convert them into UTM coordinate system (Universal Transverse Mercator). While the picture spans across path 149, line 38; path 150, line 38 and path 150, line 39. The selection of said 3 settings was based on their coverage of the research area, clarity, and absence of cloud covering. For each specific band, standard atmospheric adjustments, radiation corrections, and spatial resolution upgrades were carried out. Each individual band was combined to create a mosaic, and the study area was then masked. The adjustments were implemented with the ENVI program.

Indices Development

To determine and examine the differences in spectral reflectance between saline and non-saline soil. Mapping spectral reflectance of various soil salinity levels was crucial. This is expected to facilitate creation of soil salinity indexes. The study examined thirteen distinct spectral salinity indices that were utilized in several investigations focused on salt detection mapping and soil salinity analysis. The metrics were categorized into two subgroups: 1) Brightness or Intensity metrics and 2) Salinity Indices. The presented Tables 1 and 2 display collection of brightness or intensity and salinity indices used to create the drawings of salinity, correspondingly. In order to generate soil salinity and assess the classification of salinity levels, it is necessary to establish a particular link between the salinity index value obtained from field data and retrieved from satellite images. Consequently, the PCA investigation was conducted to establish a correlation among the field data and the indices produced from satellite images.

Table 1. Brightness or Intensity Indices for making maps of salinity

Indices	Procedure	Reference
*CRSI	$\sqrt{\frac{(NIR \times R) - (G \times B)}{(NIR \times R) + G \times B}}$	(Scudiero et al., 2015)
**NDSI	$\frac{(R - NIR)}{(R + NIR)}$	(Khan et al., 2005)
***BI-1	$\sqrt{R^2 + NIR^2}$	(Khan et al., 2005)
****BI-2	$\sqrt{G^2 + NIR^2}$	(Bouaziz et al., 2011)
*****I -1	$\frac{(G + R)}{2}$	(Bouaziz et al., 2011)
*****I -2	$\frac{(G + R + NIR)}{2}$	(Khan et al., 2005)

* Canopy Response Salinity Index; ** Normalized Differential Salinity Index; *** Brightness Index-1;

**** Brightness Index-2; ***** Intensity Index -1; ***** Intensity Index-2

Table 2. Salinity Indices used for making maps of salinity

Indices	Procedure	Reference
*SI-1	$\sqrt{G^2 + R^2 + NIR^2}$	(Nicolas and Walter, 2006)
*SI-2	$\sqrt{B \times R}$	(Khan et al., 2005)
*SI-3	$\frac{G \times R}{B}$	(Bannari et al., 2008)
*SI-4	$\sqrt{G \times R}$	(Khan et al., 2005)
*SI-5	$\frac{(B \times R)}{G}$	(Khan and Abbas, 2007)
*SI-6	$\sqrt{G^2 + R^2}$	(Nicolas and Walter, 2006)
*SI-7	$\sqrt{G + R}$	(Garcia et al., 2005)

*SI (1-7) = Salinity index 1-7

Statistical and PCA

In order to ascertain relationship, the Pearson correlation coefficient assessment was utilized to acquire insight among variables (satellite data and ground data sets), Principal Component Analysis (PCA) is a valuable method for assessing integrated multi-dimensional data. Whole spectral bands necessitate a certain level of redundancy in numbers. PCA was employed as a compression approach to address the specified problem. Principal Component Analysis (PCA) is a technique that transforms category coded variables into numerical values by optimal scaling. Linting et al., (2007) stated this process generates values and component loads from converted numeric variable. Core modules in the correlation matrix are dependent on the eigenvectors of covariance. The variance-covariance matrix CX can be presented alike;

$$C_x = \frac{1}{P - 1} \sum_{i=1}^p (X_i - M)(X_i - M)^T \dots \dots \dots (i)$$

Where, X = Variables in N dimensions with the mean vector M,

P = Number of pixel,

Every X_i component is designated by;

$$X_i = a_{1i}X_1 + a_{2i}X_2 + a_{3i}X_3 + \dots \dots \dots a_{ni}X_n \dots \dots \dots (ii)$$

The entire conversion maybe written:

$$X = A^T X \dots \dots \dots (iii)$$

Where A = matrix of eigenvectors that provides covariance matrix C_y of Y by,

$$C_y = AC_x A^T \dots \dots \dots (iv)$$

The C_y matrix = a diagonal matrix, the components that are eigenvalues of C_x is displayed as,

$$C_y = \begin{bmatrix} \lambda_1 & 0 & \dots & 0 \\ 0 & \lambda_2 & & 0 \\ \cdot & \cdot & \cdot & \cdot \\ \cdot & \cdot & \cdot & \cdot \\ \cdot & \cdot & \cdot & \cdot \\ 0 & 0 & \cdot & \lambda_n \end{bmatrix} \dots \dots \dots (v)$$

The key component method was applied to 13 NIR data sets to de-correlate redundant data, such as saline land cover, into specific PCs. For multi-spectral facts bases, PC 1 being first principal component contains of biggest ratio of complete variance and succeeding components (PC 2, PC 3,, PC 13) each variance comprise a lessening proportion of scene variance (Lillesand et al., 2015). Prior to the visual inspection of the RGB color composite, PC1s were triggered. Analyzing the Eigen-matrix can provide important insights on the structure of the original ground data and the results of the transformation. Each eigenvector may be employed to calculate the fraction of actual data variance that contributes to the creation of subsequent principal components. By examining eigenvectors for actual data, we may estimate the involvement of data to the actual PC picture (Loughlin, 1991). The red, green and blue color compound was produced (known as RGB color compound), in which PC1 of NIR is exposed in red and PC1 of Red and PC1 of Green is demonstrated in green and blue correspondingly.

RESULTS AND DISCUSSION

Utilizing several soil salinity equations can yield divergent outcomes, hence enabling the utilization of remote sensing data to accurately predict levels of soil salt on a broad gauge. The statistical correlation was produced between the salinity of soil observed in the soil samples of field and the 13 GIS-based salinity indices stated earlier. The importance of effect and the parameters of the model were tested for various soil salinity indices using regression model fitting. The facts were categorized into 3 classes: 1) Ground dataset, 2) Brightness or Intensity indices, and 3) Salinity indices. The PCA was done on the given facts. PCA is a mathematical conversion that is performed based on the examination of the correlation matrix or covariance of many spectral bands. It restructures data to eliminate interconnections and redundancies. Theoretically, it offers an intriguing approach to address the identification and detection of soil salinity, as well as determining the most relevant characteristic among all.

Spatial pattern of field data and research laboratory analysis

About 80 samples of soil were gathered from various places within the research area. The said samples were gathered from the deepness of 0-30 cm. All samples were subjected to laboratory testing to determine their pH, electrical conductivity (EC), and sodium adsorption ratio (SAR). The Table 3 presents a concise overview of the findings derived from the chemical analysis and field measurements of ground soil samples. The initial study includes the Min (minimum), Max (maximum), mean, SE (standard error), and SD (standard deviation). The analysis outcomes from the research laboratory of field facts sets are displayed in Figure 1(a), Figure 1(b), and Figure 1(c).

Power of Hydrogen (pH)

The soil pH values for the chosen data points varied from 7.7 to 10.3, with an average value of 8.83 (Table 3). The pH mapping in Figure 1(a) was conducted using IDW spatial interpolation. The results indicated that the pH levels at the research location were predominantly alkaline, with the exception of a tiny region where the soil pH was either neutral or acidic. The soil pH values vary from two to ten and are divided into six classes: Acidic (2 – 6.6), neutral (6.6 – 7.4), mildly alkaline (7.4 – 7.9), moderately alkaline (7.9 – 8.5), strongly alkaline (8.5 – 9), and very strongly alkaline i.e. > 9 (Scianna, 2002). The map indicates that the majority of the zone is characterized by moderate to very alkaline conditions, with a soil pH value above 7.9.

Electrical Conductivity (EC)

The research laboratory investigation of collected samples revealed highest and lowest values of electrical EC i.e. 65.50 & 1.30 dS m⁻¹, correspondingly (Table 3). The investigated soil salinity categorization was conducted based on the following levels: The electrical conductivity (EC) values for different types of soil are as tails: non-saline soil: 0-2 dS m⁻¹; saline-alkali soil: 2-4 dS m⁻¹; moderately saline soil: 4-6 dS m⁻¹; strongly salty soil: 6-8 dS m⁻¹; heavily saline soil: more than 8 dS m⁻¹ (Wallender and Tanji, 2011). The research findings from Figure 1(b) indicate that a significant portion of the area has moderate to very pronounced salinity issues, which may need the implementation of salinity management measures such as improved drainage or the cultivation of salt-tolerant crops. However, there are other areas within the region that exhibit either no salinity or just modest levels of salinity.

Sodium Adsorption Ratio (SAR)

The Sodium Adsorption Ratio (SAR), is a quantitative indicator of the appropriateness of soil for agricultural purposes. It is calculated by analyzing the concentration of dissolved solids, particularly sodium ions, in the soil. In general, soils with greater SAR (sodium adsorption ratio) values are less conducive to agricultural activities. Additionally, it diminishes the ability of soil to absorb and allow the passage of water, leading to complications in agricultural yield. Figure 1(c) displays the amounts of soil sodium danger. The SAR map was categorized into several classes based on the sodium adsorption ratio (SAR) values. The classifications are as follows: 0-10 (neutral), 10-18 (mildly sodic), 18-26 (moderately sodic), 26-100 (extremely sodic), and more than 100 which is very strongly sodic i.e. (Sivakumar et al., 2015). The graphic indicates that the majority of the study region has SAR values over 18, indicating moderately to very highly sodic conditions. Table 3 displays the SAR values, which vary from 6.60 to 290.10, with an average of 54.14.

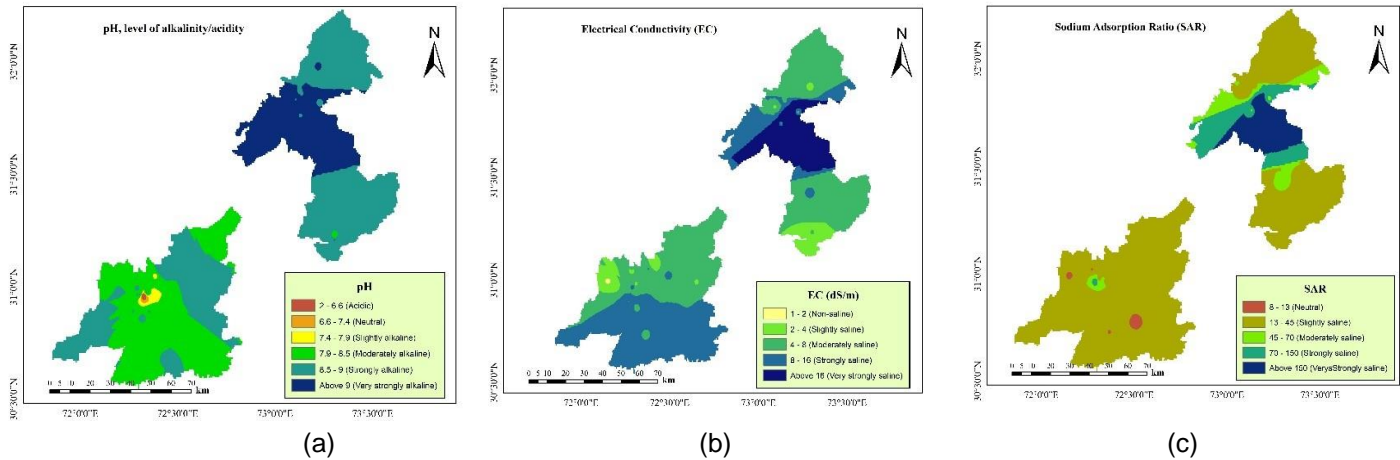


Figure 1. Soil pH (a), EC (b), and SAR (c) taken from exclamation of research location observation data

Table 3. Laboratory analysis of soil samples

Factors	N	*Depth	Range	Min	Max	Mean		SD
						Statistic	SE	
pH	80	0 – 30	2.6	7.7	10.3	8.83	0.0724	0.6474
EC	80	-do-	64.2	1.3	65.5	10.19	1.4018	12.5379
SAR	80	-do-	283.5	6.6	290.1	54.15	7.8436	70.1551

*Depth was measured in cm

Spatial Pattern of Varied RS Based Soil Salinity Indices

The soil samples spectral reflectance were analyzed over certain wavelength ranges, including the visible range (400-770 nm) and near-infrared (NIR) range (900-1030, 1270-1700, 1900-2150, 2150-2310, 2320-2400). The references used are and Sidike et al., (2014) and Nawar et al., (2014). The spectral absorption pattern is closely linked to level of salt and has been used to quantitatively assess soil salinity by remote sensing (RS). Though, the spectral features were primarily influenced by the existence of vegetation and soil crust, which altered the soil texture and resulted in a solid reflecting impact on visible and near-infrared electromagnetic waves. This reflection was greater than that observed in moderately or non-saline soil. The reflection level is closely correlated with the degree of saline within soil (Bouaziz et al., 2011).

Several salinity indexes have been produced in various research studies. The analysis of soil salinity involved the examination of salt buildup and the mapping of salinity using Landsat imagery. Thirteen salinity indices, which are listed in Table 1 and Table 2, were considered in this research. The broadband indicators were selected based on their relevance in determining soil salinization. The indicators were categorized into 2 distinct classes: i) Brightness or Intensity indicators (NDSI, CRSI, BI-1 & 2, II-1 & 2) and ii) Salinity Indices (SI-1 to 7). These classifications are illustrated in Figures 2 and 3 correspondingly.

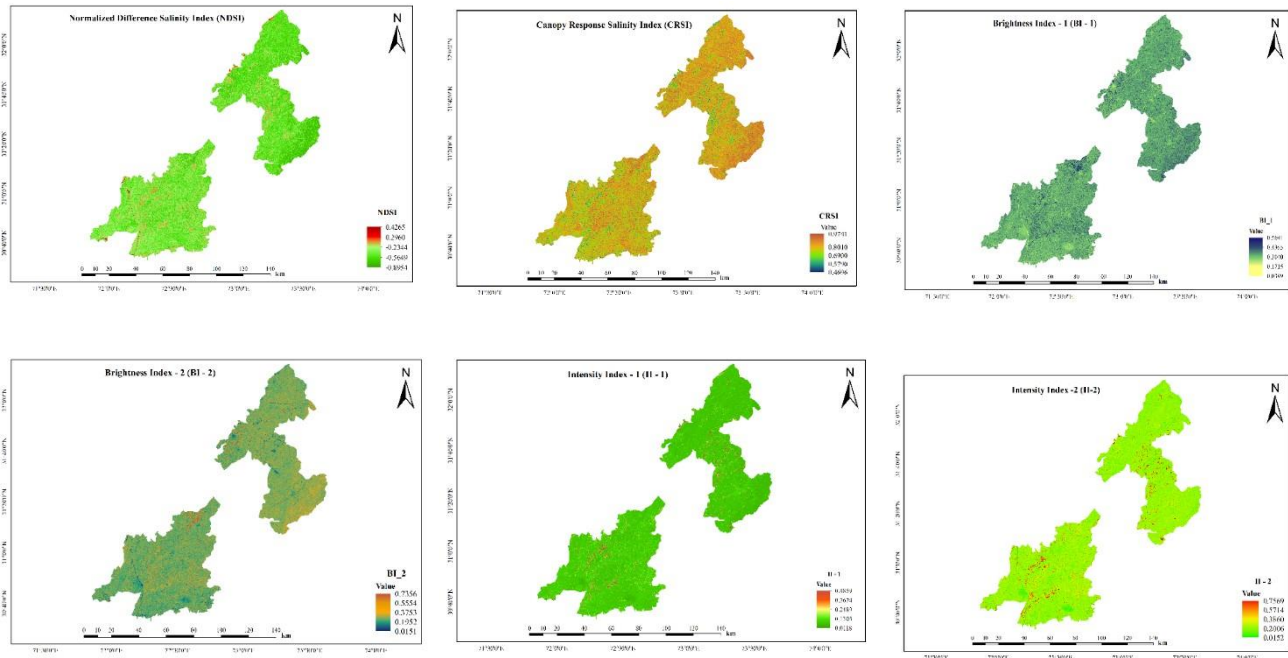


Figure 2. Brightness or Intensity Indices maps of the research site created through Landsat 8 OLI

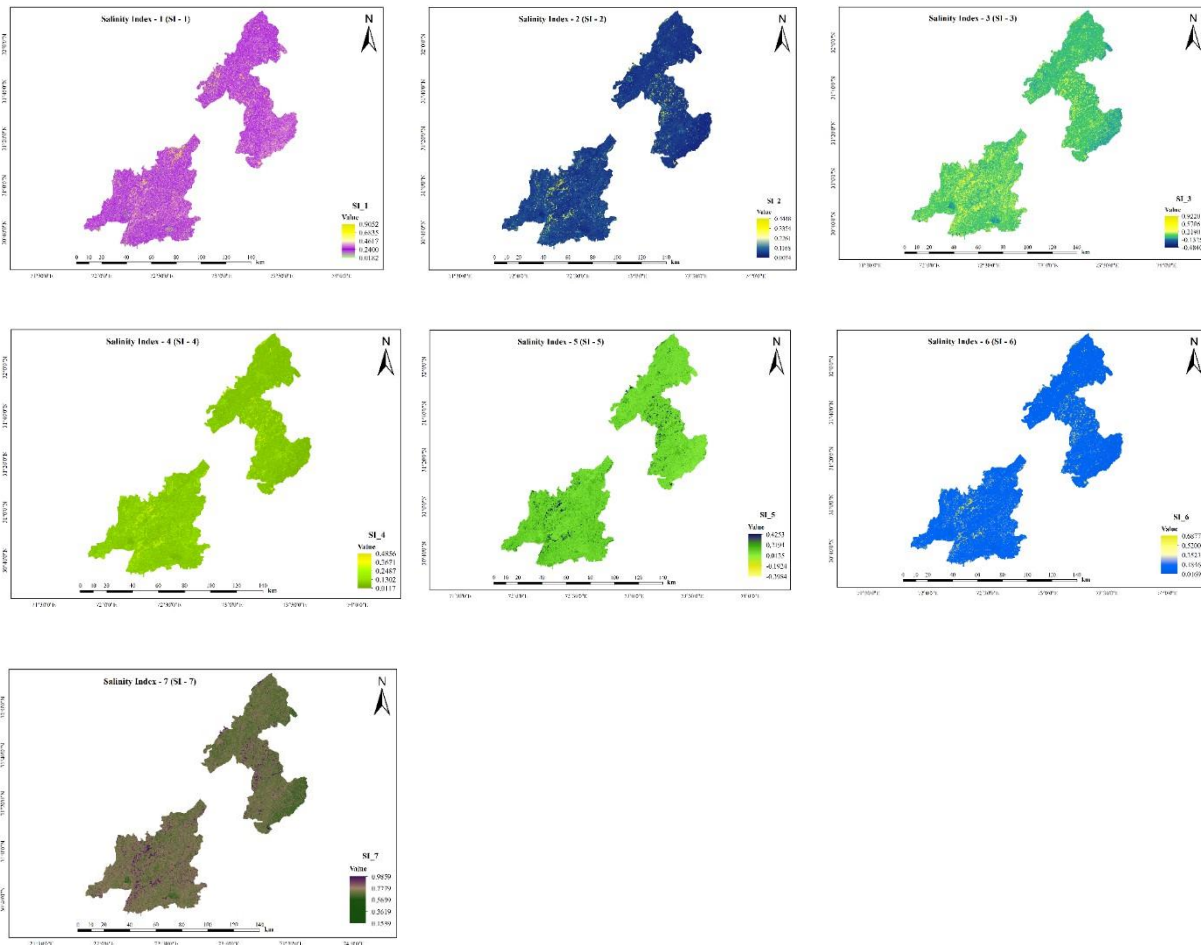


Figure 3. Salinity Indices maps of the research site created from Landsat 8 OLI

Based on the survey samples in this study, it was shown that very saline soils have a more pronounced spectral response in the visible and near-infrared region compared to lower degrees of salt. The presence of crystalline salts on the surface of very saline soils significantly contributes to the overall spectral reflectance of the surface. The findings of Allbed et al., (2014), and Everitt et al., (1988), are consistent with these results. They discovered that soils with well-developed salt weathering and crusts had high reflectance in both visible and NIR wavelengths. The presence of well-structured soils with high organic matter content is believed to contribute to a decrease in spectral reflectance. This conclusion is reliable with the study conducted by Bannari et al., (2008).

Furthermore, this study reveals that soil salinity affects the spectral reflectance of different types of salt bark surfaces. The soft, dry and less coloured salt bark tops exhibit more spectral reflectance in visible part of spectrum, particularly in the red band. On the other hand, saline soils with wetness, hardness, and dark fuzzy salt surface show less spectral reflectance. The outcomes align with the conclusions of Fallah et al., (2013), who demonstrated that reflectivity of salty soils is influenced by various spectral characteristics, including the existence of salt surfaces, moisture content, color, and roughness. These characteristics collectively contribute to the overall reflectivity of the soil.

Connection Among Field Data and Soil Salinity Indices

The correlation investigation presented in Table 4 revealed that associations between the field data sets (pH, EC, SAR) and chosen salinity indices were distinct. When evaluating soil salinity, the pH, NDSI, II-1, SI-4 & 6 indices were found to be the only relevant indicators. However, when considering EC, NDSI, CRSI, II-1, SI-6 & 7 were identified as the suitable soil salinity indices. Similarly, when it comes to SAR, the variables II-1, SI-4, and SI-6 exhibit the most robust and statistically significant association. However, some studies have found strong connections among field data sets and several soil salinity indicators (Wang et al., 2020; Bouaziz et al., 2011). The decent representation of the NDSI, CRSI, II-1, SI-6 & 7 indices yields similar results to those obtained from red, NIR, blue, and green bands, which employed to capture the salinity outlines and features such as the top soil crust. The correlation between the red and NIR spectral areas has been observed as a means of recognizing stress by salts including various soil minerals found in the crust (Zhang et al., 2011). These findings are corroborated by Wang et al., (2020) and Allbed et al., (2014), who noted that the CRSI and NDSI indices provide satisfactory results in defining different levels of salt extent on the soil surface. However, the outcomes from the research of Bannari et al., (2008) shown that the NDSI is not a reliable sign of salty content.

Table 4. Correlation coefficients among EC, pH and SAR and satellite based Salinity values

Factor	EC		pH		SAR	
	Cor. Coeff	p value	Cor. Coeff	p value	Cor. Coeff	p value
CRSI	-0.78	0.01	-0.39	0.60	-0.51	0.20
NDSI	-0.65	0.01	-0.75	0.01	-0.43	0.46
BI-1	0.48	0.68	0.47	0.79	0.44	0.79
BI-2	0.46	0.88	0.41	0.70	0.42	0.61
II-1	0.59	0.01	0.60	0.01	0.60	0.01
II-2	0.58	0.75	0.57	0.17	0.56	0.19
SI-1	0.54	0.95	0.51	0.44	0.51	0.65
SI-2	0.58	0.97	0.60	0.96	0.58	0.39
SI-3	0.55	0.69	0.58	0.57	0.57	0.62
SI-4	0.59	0.08	0.60	0.01	0.59	0.01
SI-5	0.56	0.91	0.59	0.89	0.56	0.59
SI-6	0.59	0.01	0.60	0.01	0.60	0.01
SI-7	0.56	0.01	0.59	0.73	0.58	0.82

Principle Component Analysis

Dataset include both ground-based and the satellite-derived soil salinity data and/ or indicators. Oftentimes, there is duplication in the obtained data, leading to correlation between variables. It is advisable in this situation to employ data reduction techniques to decrease the large collection of variables to a more concise and essential set of variables. Keho (2012) recommends using Principal Component Analysis (PCA) for generating indexes.

The Principal Component Analysis (PCA) yielded three components when applied to the ground data, six components when applied to the brightness/intensity indices, and seven components when applied to the salinity indices. These components account for 83%, 70%, and 93% of the total variance, respectively (Table 5). The Bartlett and KMO tests produced comparable findings in the principal component analysis of the first two components. The KMO test yielded a value of 0.79, whereas Bartlett's test of sphericity displayed a statistical significance of less than 0.01.

According to the Kaiser (1960) criteria, only components with eigenvalues greater than 1 are used in constructing the PCA. Therefore, the components for the field data set, brightness or intensity, and salinity indices with eigenvalues of 2.49, 4.22, and 6.55 correspondingly are used in the PCA creation by use of below procedure. To generate an index for salinity conduct, square of the values in column 3 of Table 5 is multiplied by the replies of individuals for identifications of salinity in succeeding mode (Equation vi, vii & viii);

$$PCA_{Ground\ data} = pH \times 0.54^2 + EC \times 0.57^2 + SAR \times 0.60^2 \dots \dots (vi)$$

$$PCA_{BI} = NDSI \times -0.32^2 + CRSI \times -0.33^2 + BI1 \times 0.42^2 + BI2 \times 0.39^2 + II1 \times 0.46^2 + II2 \times 0.47^2 \dots \dots (vii)$$

$$PCA_{SI} = si1 \times 0.33^2 + si2 \times 0.38^2 + si3 \times 0.37^2 + si4 \times 0.39^2 + si5 \times 0.38^2 + si6 \times 0.39^2 + si7 \times 0.38^2 \dots \dots (viii)$$

The results indicate that, when considering field data, only one out of the three components has an Eigen value greater than 1. Put simply, only component 1 meets the requirements set by Kaiser (1960) for it to be included in the PCA. Likewise, for brightness/ intensity indices, two out of six components have Eigen values more than 1. However, for salinity indices, only one out of seven components has an Eigen value greater than 1. A series of ordinary least squares (OLS) regressions were conducted to assess the impact of various ground data sets on satellite-based salinity indicators. The comprehensive outcomes of the inquiry are succinctly outlined in Table 6. The results indicate a positive correlation between salinity indicators and the ground data sets. The ground data exhibits a consistent and predictable pattern of change in response to variations in salinity indices, and this relationship is statistically significant at a 1% level of confidence. The monotonic relationship remains stable throughout all 3 constituents of the index, with minimal change in value of coefficient. The brightness or intensity indices do not show a meaningful correlation with the sets of ground numbers.

Table 5. PCA results for Field data sets, Brightness or Intensity and salinity indices

Data Sets	Component	Factor loadings
Field Data Eigen value 2.49 Variance described 83%	pH	0.54
	EC	0.57
	SAR	0.60
Brightness or Intensity Indices Eigen value 4.22 variance described 70%	NDSI	-0.32
	CRSI	-0.33
	BI-1	0.42
	BI-2	0.39
	II-1	0.46
	II-2	0.47
Salinity indices Eigen value 6.5 variance described 93%	SI-1	0.33
	SI-2	0.38
	SI-3	0.37
	SI-4	0.39
	SI-5	0.38
	SI-6	0.39
	SI-7	0.38

CONCLUSION

Results concluded that application of remote sensing followed by field observation is a powerful tool for detecting saline areas. Indices like NDSI, II-1, SI-4, SI-6, and SI-7 is the good to present soil salinity values in the present research zone. Monitoring temporal soil salinity study are the major investigation adequate natural resource management plan in the immediate upcoming. While this research showed that soil salinity mapping and modeling can be performed well based on high spatial resolution multispectral images but additional study is still desirable to

investigate the hyperspectral data in areas dominated by different crops. Possibility of salt mapping and modeling investigate whether it can improve the accuracy of the modeling and mapping process.

ACKNOWLEDGEMENTS

We thank the all authors specifically Dr. Ali Raza Siddiqui while working on writing original draft, review, editing and final submission.

AUTHOR CONTRIBUTIONS

All authors contributed equally to this research.

COMPETING OF INTEREST

No conflicts of interest have been disclosed by the authors.

REFERENCES

- Al-Khaier, F. 2003. Soil salinity detection using satellite remote sensing. ITC. M.Sc. Thesis. The International Institute for Geo-Information Science and Earth Observation. Enschede, Netherlands. *Adv. Remote. Sens.* 6: 1.
- Allbed, A., Kumar, L., Aldakheel, Y.Y. 2014. Assessing soil salinity using soil salinity and vegetation indices derived from IKONOS high-spatial resolution imageries: Applications in a date palm dominated region. *Geoderma*, 230. pp.1–8.
- Anjum, S., Mustaq, Z., Sarwar, M., et al 2024. Climate change and its impact on agriculture. *J. Agric. Biol* 2(1). pp.84–103.
- Anjum, S., Sarwar, M., Mukhtar, A., et al 2025. Impact of rhizobacterial inoculation in plant growth medium to mitigate lead stress in Tomato (*Solanum lycopersicum* L.). *Sci. Rep* 15(1). pp.707.
- Anjum, S., Qurat-ul Ain, M., Sarwar, M., et al 2025. Chitosan induced modification in morpho-physiological, biochemical and yield attributes of pea (*Pisum sativum* L.) under salt stress. *J Soil Sci Plant Nutr.*
- Bannari, A., Guedon, A.M., El-Harti, A., et al 2008. Characterization of slightly and moderately saline and sodic soils in irrigated agricultural land using simulated data of advanced land imaging (EO-1) sensor. *Commun. Soil Sci. Plant Anal* 39(19–20). pp.2795–2811.
- Bouaziz, M., Matschullat, J., Gloaguen, R. 2011. Improved remote sensing detection of soil salinity from a semi-arid climate in Northeast Brazil. *Comptes Rendus Geoscience* 343(11–12). pp.795–803.
- Bouman, B.A.M., Tuong, T.P. 2001. Field water management to save water and increase its productivity in irrigated lowland rice. *Agric. Water Manag* 49(1). pp.11–30.
- De Boer, H.C., Radersma, S. 2011. Verzilting in Nederland: oorzaken en perspectieven (No. 531). Wageningen UR Livest. Res.
- Eldeiry, A., Garcia, L. 2004. Spatial modeling using remote sensing, GIS, and field data to assess crop yield and soil salinity. *Hydrol. Days* 7. pp.55–66.
- Elhag, M., Bahrawi, J.A. 2017. Soil salinity mapping and hydrological drought indices assessment in arid environments based on remote sensing techniques. *Geoscientific Instrumentation, Methods and Data Systems* 6(1). pp.149–158.
- Estes, J.E., McGWIRE, K.C., Fletcher, G.A., et al 1987. Coordinating hazardous waste management activities using geographical information systems. *Int. J. Geogr. Inf. Sci* 1(4). pp.359–377.
- Escobar, D.E., Gerbermann, A.H., Alaniz, M.A. 1988. Detecting saline soils with video imagery.
- Fallah Shamsi, S.R., Zare, S., Abtahi, S. A. 2013. Soil salinity characteristics using moderate resolution imaging spectroradiometer (MODIS) images and statistical analysis. *Arch. Agron. Soil Sci* 59(4). pp.471–489.
- Farifteh, J., Farshad, A., George, R.J. 2006. Assessing salt-affected soils using remote sensing, solute modelling, and geophysics. *Geoderma*, 130(3-4). pp.191–206.
- Fussell, J., Rundquist, D., Harrington, J. A. 1986. On defining remote sensing. *PE&RS* 52(9). pp.1507–1511.
- Garcia, L., Eldeiry, A., Elhaddad, A. 2005. Estimating soil salinity using remote sensing data. In *Proceedings for the 2005 Central Plains Irrigation Conference, Sterling, Colorado, February 16–17*. Colorado State University Libraries.
- Hillel, D. 2000. *Salinity management for sustainable irrigation: integrating science, environment, and economics*. World Bank Publications.
- Hussain, N., Sarwar, G., Schmeisky, H., et al 2010. Salinity and drought management in legume crops. *Climate change and management of cool season grain legume crops*, pp.171–191.
- Kaiser, H. F. 1960. The application of electronic computers to factor analysis. *Educational and Psychological Measurement*, 20(1). pp.141–151.
- Keho, Y. 2012. The basics of linear principal components analysis. *Principal Component Analysis*, Parinya Sanguansat, IntechOpen.

- Khan, N.M., Rastoskuev, V.V., Sato, Y., et al 2005. Assessment of hydrosaline land degradation by using a simple approach of remote sensing indicators. *Agric. Water Manag* **77**(1–3). pp.96–109.
- Abbas, A., Khan, S. 2007. Using remote sensing techniques for appraisal of irrigated soil salinity. *MODSIM* pp.2632–2638. Modelling and Simulation Society of Australia and New Zealand.
- Lillesand, T., Kiefer, R. W., Chipman, J. 2015. *Remote sensing and image interpretation*. John Wiley & Sons. pp.485–486.
- Linting, M., Meulman, J.J., Groenen, P.J. 2007. Nonlinear principal components analysis: introduction and application. *Psychological Methods*, **12**(3). pp.336.
- Loughlin, W.P. 1991. Principal component analysis for alteration mapping. *PE&RS* **57**(9). pp.1163–1169.
- Martin, P., Nishida, J., Afzal, J., et al 2006. Pakistan strategic country environmental assessment. South Asia Region, World Bank. pp.1–80.
- Sarwar, M., Amjad, M., Ayyub, C.M. 2017. Alleviation of salt stress in cucumber (*Cucumis sativus* L.) through seed priming with triacontanol. *Int. J. Agri. Bio* **19**. pp.771–778.
- Sarwar, M., Anjum, S., Khan, M.A., et al 2018. Assessment of sustainable and eco-friendly agricultural substrates for eminence production of chilies for kitchen gardening. *Int J Recycl Org Waste Agriculture* **7**. pp.365–374.
- Sarwar, M., Amjad, M., Anjum, S., et al 2019a. Improving the salt stress tolerance in cucumber (*Cucumis sativus* L.) using triacontanol. *JHST* **2**(1). pp.20-26.
- Sarwar, M., Ahmad, S., Chattha, M.B., et al 2019b. Assessment of growth and productivity of cucumber (*Cucumis sativus* L.) genotypes under salt stress regime. *Appl. ecol. environ. res* **17**(5). pp.10793-10806.
- Sarwar, M., Anjum, S., Alam, M.W., et al 2022. Triacontanol regulates morphological traits and enzymatic activities of salinity affected hot pepper plants. *Sci Rep* **12**. pp.3736.
- Sarwar, M., Anjum, S., Ali, Q., et al 2021. Triacontanol modulates salt stress tolerance in Cucumber by altering physiological and biochemical status of plant cell. *Sci Rep* **11**, p.24504.
- Nawar, S., Buddenbaum, H., Hill, J. 2014. Modeling and mapping of soil salinity with reflectance spectroscopy and Landsat data using two quantitative methods (PLSR and MARS). *Remote Sense* **6**(11). pp.10813-10834.
- Nicolas, H., Walter, C. 2006. Detecting salinity hazards within a semiarid context by means of combining soil and remote-sensing data. *Geoderma* **134**(1-2). pp.217-230.
- Pakistan Meteorological Department, 2018. Climate Data Processing Centre.
- Rahman, S., Munn, L.C., Vance, G.F., Arneson, C. 1997. Wyoming Rocky Mountain forest soils: mapping using an ARC/INFO geographic information system. *SSSAJ* **61**(6). pp.1730-1737.
- Scianna, J., 2002. Salt-affected soils: their causes, measure, and classification. *Res. Method Hort. Note*, **5**. pp.1-3.
- Scudiero, E., Corwin, D.L. 2015. Regional-Scale Soil Salinity Assessment Using Landsat ETM+. *ASA, CSSA and SSSA International Annual Meetings*.
- Shahid, S.A., Zaman, M. 2018. Soil salinity: Historical Perspective and a World Overview of the Problem. *Guideline for Salinity Assessment, Mitigation and Adaptation Using Nuclear and Related Techniques. Springer Cham*. pp. 43–53.
- Sidike, A., Zhao, S. 2014. Estimating soil salinity in Pingluo County of China using QuickBird data and soil reflectance spectra. *Int. J. Appl. Earth Obs. Geoin*, **26**. pp. 156-175.
- Sivakumar, D., Pavithra, S.L. 2015. Groundwater suitability for irrigation around Perungalathur, Chennai, Tamil Nadu. *Int. J. Appl. Eng. Res* **10**(53),
- Song, Y., Guo, Z., Lu, Y., et al 2017. Pixel-level spatiotemporal analyses of vegetation fractional coverage variation and its influential factors in a desert steppe: A case study in Inner Mongolia, China. *Water* **9**(7), 478.
- Tajgardan, T., Ayoubi, S., Shataee, S., et al 2010. Soil surface salinity prediction using ASTER data: Comparing statistical and geostatistical models. *Aust. j. basic appl. sci* **4**(3). Pp. 457-467.
- Unwin, D. J. 1996. GIS, spatial analysis and spatial statistics. *Progress in Human Geography*, **20**(4). pp. 540-551.
- Wallender, W.W., Tanji, K.K. 2011. *Agricultural Salinity Assessment and Management*. 2nd Ed. American Society of Civil Engineers, Reston, Virginia, USA.
- Wang, F., Shi, Z., Biswas, A., et al 2020. Multi-algorithm comparison for predicting soil salinity. *Geoderma* **365**, 114211.
- Zhang, T.T., Zeng, S.L., Gao, Y., et al 2011. Using hyperspectral vegetation indices as a proxy to monitor soil salinity. *Ecol. Indic* **11**(6), pp.1552-1562.